文章编号：1001－9014(2016)02－0139－04

DOI:10.11972/j.issn.1001－9014.2016.02.003

Photocurrent and responsivity of quantum dot infrared photodetectors

LIU Hong-Mei[1,2*], WANG Ping[1,2], SHI Yun-Long[1,2]

(1. Institute of Solid State Physics, Datong University, Datong China;
2. School of Physical Science and Electronics, Datong University, Datong China)

Abstract: In this paper, a model for the photocurrent of the quantum dot infrared photodetector (QDIP) including the continuous potential distribution of the electrons and the total electron transport is improved with the consideration of the dependence of the photoconductive gain on the applied bias, and this improved model can be further used to estimate the responsivity of the photodetector. The corresponding calculated results show a good agreement with the published results, which verifies the validity of the improved model.

Key words: quantum dot infrared photodetectors (QDIP), photocurrent, responsivity, photoconductive gain
PACS: 85.35.Be, 07.57.Kp, 85.60.Gz, 07.50.HP

量子点红外探测器的光电流和响应率

刘红梅[1,2*], 王 萍[1,2], 石云龙[1,2]
(1. 山西大同大学 固体物理研究所,山西 大同 037009;
2. 山西大同大学 物理与电子科学学院,山西 大同 037009)

摘要:通过考虑光电导增益对探测器所加电压的依赖性改进了包含电子持续势能和总电子传输的光电流模型,并进一步将这个改进的模型用于估算探测器的响应率.相应的计算结果与公布的结果相比较,具有很好的一致性,证明了改进模型的正确性.

关 键 词:量子点红外探测器;光电流;响应率;光电导增益

中图分类号:TN215 **文献标识码**:A

Introduction

The photocurrent and the responsivity of quantum dot infrared phototdetectors, which describe the ability of the photodetecor to detect the infrared light, have been the focus of attentions since 1999[1-2], at the same time, their corresponding physical models have also become hot topics.[3-4] In 2009, A. Rogalski and his co-workers proposed the physical model of the quantum dot infrared photodetectors (QDIP) with the consideration of the continuous potential distribution and the emission of the electrons[5], and this model was used to estimate the photocurrent, the responsivity and so on. In 2010, L. Lin pointed out that the total electron transport of the QDIP included the microscale and the nonascale electron transport [6]. Based on this theory, the previous model of the QDIP built by A. Rogalski was improved with the consideration of the influences of the total electrons transport and the electrons continuous potential distribution in 2012[7]. Though these models can well estimate performances of the QDIP, the photoconductive gain was assumed as the constant in their calculations, and the responsivity wasn't further calculated. In fact, the influence of the bias voltage on the photoconductive gain should be considered in the photocurrent calculation due to its great dependence on the electric field[8-9]. According to this theory, in the paper, the photocurrent model including the contribution of the electrons continuous potential distribution and the total electron transport is improved with the consideration of the dependence of the photoconductive gain on the bias voltage, and the model of the responsivity is further derived. The corresponding calculated results are given to show the validities of our

Received date: 2014 - 10 - 20, **revised date**: 2015 - 10 - 06 **收稿日期**:2014 - 10 - 20, **修回日期**:2015 - 10 - 06
Foundation items:Supported by Launching Scientific Research Funds for Doctors (2012-B-04), National Natural Science Foundation of China(61307121, 11274207),Industry Research Prroject of Datong City(2015018) and Aeronautical Science Foundation of China (20122481002)
Biography:LIU Hong-Mei(1980-),female, Ph. D. Research interests include the performance characterization of the infrared photodetector and nano optoelectronicdevice. E-mail: lhm9898@163.com
* **Corresponding author**:E-mail:lhm9898@163.com

improved model.

1 Model

As shown in Fig. 1, the QDIP device consists of many periods of the quantum dots layers including many identical quantum dots, the barrier layers, the top and the bottom contacts(corresponding to the emitter and the collector, respectively). Here, each quantum dot is supposed as large enough in the lateral size and very small in the transverse size, so it can provide with a large number of bound states to accept more electrons in the lateral direction and with the single energy level in the transverse direction, respectively. Based on above assumptions, the photocurrent model including the total electrons transport and the continuous potential distribution is improved by considering the influence of the electric field on the photoconductive gain, and it is further used to estimate the responsivity of the QDIP.

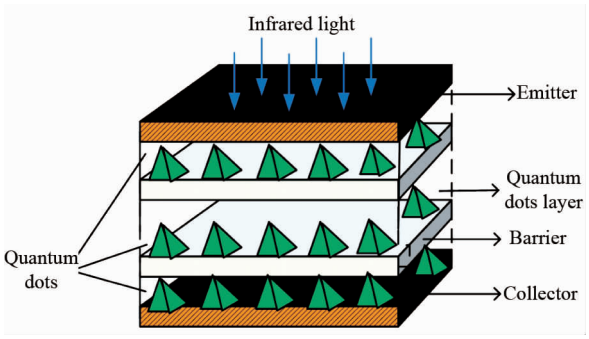

Fig. 1 Schematic view of QDIP layers structure
图1 量子点红外探测器层结构示意图

1.1 Photocurrent model

As well known to us, the photocurrent of the QDIP, which is defined as the current of the photodetector under an illumination condition, can be determined by the following Eq. 1.

$$I_{\text{photo}} = e\Phi_s \eta g_p A_d \quad , \quad (1)$$

where e is the electron charge, Φ_s is the incident photo flux density on a detector, η is the quantum efficiency, A_d is the area of the photodetector, and g_p is the photoconductivity gain.

In the QDIP, the quantum efficiency can be obtained as[5]:

$$\eta = \delta < N > K\sum_{\text{QD}} \quad , \quad (2)$$

where δ is the electron capture cross section coefficient, K is the total layer number of the quantum dots layer, $\sum_{QD}$ is the density of the quantum dots in a quantum dot layer, $<N>$ is the average number of the electrons in a quantum dot, which can be obtained by the current balance relation under the dark condition. Concretely speaking, the dark current can be obtained by counting the mobile carriers in the barrier[10-11]. At the same time, it is also pointed out that those currents that flow the punctures in the planar potential barriers together form the dark current of the total QDIP device[12]. Hence, the current balance relation in the dark conditions can be written as:

$$2evA_d\left(\frac{m_b k_B T}{2\pi\hbar^2}\right)^{3/2}\exp\left(-\frac{E_{0,\text{micro}}\exp(-E/E_0)+E_{0,\text{nano}}-\beta E}{k_B T}\right) = A^* T^2 A_d \frac{\Theta}{<N>}\exp\left[e\frac{V+V_D-(<N>/N_{\text{QD}})V_{\text{QD}}}{(K+1)k_B T}\right] \quad , \quad (3)$$

where v is the drift velocity of electrons, m_b is the effective mass of the electron, k_B is the Boltzmann constant, T is the temperature, $\hbar$ is the reduced Planck constant, E is the electric field intensity, $E_{0,\text{micro}}$, $E_{0,\text{nano}}$, E_0 and β are the parameters related to the activation energies under the microscale and the nanoscale transport, A^* is the Richardson constant, the parameters Θ, V_{QD}, V_{D}, ϑ are dependent on the structure and the materials of the QDIP.

By solving Eq. 3, we can get the average number of the electrons in a quantum dot $<N>$ and obtain the quantum efficiency. Based on this calculation of the quantum efficiency, the photocurrent can be obtained after Eq. 2 is substituted into Eq. 1, and its expression can be written as:

$$I_{\text{photo}} = e\delta g_p <N> \sum_{\text{QD}} \Phi_s K A_d \quad . \quad (4)$$

From Eq. 4, it can be found that, in the above photocurrent model, the photoconductive gain is supposed as the constant, but in fact, the photoconductive gain strongly depends on the electric voltage. This dependence should be included in the photocurrent calculation[5,8-9]. Hence, in our model, the influence of the applied bias on the photoconductive gain is considered to enhance the precision of the photocurrent calculation.

In the QDIP, under the condition that the capture probability is small and the transit time across one period of the quantum dot composite layer is considerably smaller than the recombination time from an extended state back into a quantum dot, the photoconductive gain can be calculated as[5,8]:

$$g_p = \frac{1}{Kp_k} = \frac{N_{\text{QD}}}{KP_{0k}(N_{\text{QD}}-<N>)\exp\left(-\frac{\pi\sqrt{\pi}e^2<N>}{2\varepsilon_r\varepsilon_0 a_{QD}kT}\right)} \quad , \quad (5)$$

where p_k is the neutral capture probability, P_{0k} is the capture probability for the uncharged quantum dots, and a_{QD} is the lateral dimension of the quantum dot.

Substituting Eq. 5 into Eq. 4, we can get the photocurrent which is shown as :

$$I_{\text{photo}} = \frac{\delta e N_{\text{QD}} <N> \sum_{\text{QD}} \Phi A_d}{P_{0k}(N_{\text{QD}}-<N>)\exp\left(-\frac{\pi\sqrt{\pi}e^2<N>}{2\varepsilon_0\varepsilon_r a_{\text{QD}}kT}\right)} \quad . \quad (6)$$

1.2 Responsivity

The current responsivity is defined as the output photocurrent of the photodetector per the input power, and it can be obtained as:

$$R_i = \frac{I_{\text{photo}}}{\Phi_s h\nu_0} \quad . \quad (7)$$

Substituting Eq. 6 into Eq. 7, we can get the responsivity of the QDIP, which is shown as:

$$R_i = \frac{\delta e N_{QD} < N > \sum_{QD} A_d}{h v_0 P_{0k} (N_{QD} - < N >) \exp\left(- \frac{\pi \sqrt{\pi} e^2 < N >}{2 \varepsilon a_{QD} k T} \right)} . \quad (14)$$

2 Simulation and data

The photocurrent and the responsivity of the QDIP are simulated and calculated in this section. The corresponding calculated results are compared with the experimental results reported in the literatures to verify the validity of our model. Here, in order to make the verification clearer, the experimental results are transferred from the voltage coordinates into the electric field intensity coordinates. Table 1 shows the parameters values of the QDIP in our simulations and calculations. Specifically, the incident photo flux density Φ_s is supposed as 8×10^{17} photons/cm^2s, and the other parameters are adjusted to the same values as those of the GaAs or InGaAs QDIP devices[5-7,13-14] used to the verification of our model.

Table 1　Parameters of QDIP devices

表 1　量子点红外探测器器件参数

$E_{0,\text{micro}} = 34.6$ meV	$E_0 = 1.62$ kV/cm	$K = 10$
$E_{0,\text{nano}} = 224.7$meV	$\beta = 2.79$ meVcm/kV	$N_{QD} = 8$
$\Sigma_{QD} = (1\text{-}4) \times 10^{10}$ cm^{-2}	$L = 59\text{-}61.5$ nm	$\varepsilon_r = 12$
$v = 2 \times 10^5$ m/s	$A_d = 100 \times 100 - 300 \times 300$ μm^2	$\Sigma_D = 0.3$ Σ_{QD}
$a_{QD} = 20$ nm	$m_b = .023$ m_e	$P_{0k} = 1$

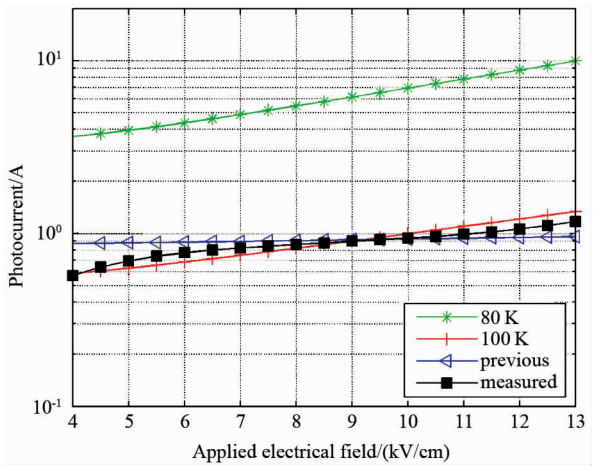

Fig. 2　Photocurrent as function of applied electric field

图 2　函数变量为应用电场的光电流

Figure 2 presents the photocurrent as functions of the applied electrical field. In this figure, the curve including the triangles indicates the photocurrent data at 100 K from the previous photocurrent model, the curve with '+' represents the photocurrent values at 100 K from our improved photocurrent model, and those photocurrent values including "black squares" are the experimental data at the same temperature from the QDIP device, which is made up of 0.5 μm GaAs top contact, a ten-period stack of 30nmGaAs/3ML InAs Quantum Dots and 1 μm GaAs bottom contact[13]. By making a comparison between our photocurrent results and the previous photocurrent data, it can be clearly found that, our photocurrent results are smaller than the previous photocurrent data below the electric field 6.5 kV/cm and they are higher than the previous data upon the electric field 12 kV/cm. The difference leads to the better consistence between our results and the experimental data than that between the previous photocurrent results and the experimental data. Such consistency not only indicates that the photocurrent calculation in our model is more precise than that in the previous model, but also shows the correctness and the validity of our model. In addition, it can be seen that these photocurrent curves show the increase trends with increasing of the electric field. For example, in the curve "100 K", the photocurrent increases from 0.682 A to 1.21 A when the electric field density is increased from 6 kV/cm to 12 kV/cm. This change of the photocurrent clearly illustrates the influence of the electric field density on the photocurrent. The similar increase trend of the photocurrent can be seen in the other photocurrent curves. From the physical mechanism point of view, the increased electric field brings about the enhanced reduction of the potential barrier. More electrons possibly escape from the quantum dots over this reduced barrier, thus the large photocurrent can be obtained.

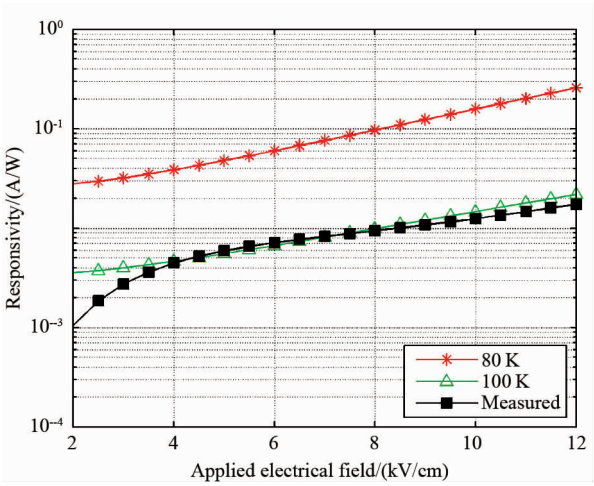

Fig. 3　Responsivity as functions of applied electric field

图 3　函数变量为应用电场的响应率

Figure 3 presents the responsivity values of the QDIP. In this figure, the curves with "*" and "Δ" represent the responsivity results from our model at the temperature of 80 K and 100 K, respectively, and the curve including the black squares indicates the experimental values at 100 K from the QDIP device including the ten-period 4 nm$Al_{0.1}Ga_{0.9}As$ /4 nmGaAs /$In_{0.4}Ga_{0.6}$AsQDs /1 nmGaAs /3 nm $Al_{0.3}Ga_{0.7}As$/4 nm $In_{0.1}Ga_{0.9}$As/3 nm$Al_{0.3}Ga_{0.7}As$/40 nm GaAs[14]. At the temperature 100 K, it is very clear that our responsivity results agree with the published experimental results, which well examines the validity of our models. In addition, just as shown in the curve "80 K", the electric field makes a great contribution to the responsivity. For example, the responsivity is only 3.85×10^{-2} A/W under the electric field density 4 kV/cm, and then it rapidly reaches to

2.58×10^{-1} A/W when the electric field is increased to 12 kV/cm, which is about 1 order of magnitude larger than that at 4 kV/cm. The reseponsivity curve "100 K" also shows the similar increase from 4.63×10^{-3} A/W to 2.18×10^{-2} A/W within the electric field range 4 kV/cm ~12 kV/cm. The increase of the responsivity can be ascribed to the increasing of the photocurrent and the electric field.

3 Conclusions

In the paper, the photocurrent model of the QDIP including the total electron transport and the continuous potential distribution of the electrons is improved by accounting for the influence of the bias voltage on the photoconductive gain. The responsivity is further calculated on the basis of this improved model. The corresponding results agree with the published experimental results, and such agreement tests and verifies the accuracy of our model.

Acknowledgments

The work was supported by Launching Scientific Research Funds for Doctors ('Research on characteristics of Quantum dots Infrared Photodetectors', Grant NO. 2012-B-04), National Natural Science Foundation of China('Performance estimation of Quantum dots infrared Photodetectors', Grant No. 61307121 & 'Research on Photon transfer behaviour in Grapheme-like Zero Refractive Index Metamaterials', No. 11274207), Industry Research Prroject of Datong City('Research on high and photoelectric performance film materials with quantum-dots nanostructure', No. 2015018) and Aeronautical Science Foundation of China ('Research on Technology in Infrared Detector Virtual Prototype', Grant No. 20122481002).

References

[1] Phillips J, Bhattacharya P, Kennerly S W, *et al*. Self-assembled InAs-GaAs quantum-dot intersubband detectors[J]. *IEEE Journal of Quantum Electctronics*, 1999, **35**:936-943.

[2] Carbone A, Introzzi R, Liu H C. Photo and dark current noise in self-assembled quantum dot infrared Photodetectors[J]. *Infrared Physics & Technology*, 2009, **52**: 260-263.

[3] Dehdashti Jahromi H, Hossein Sheikhi M, Hasan Yousefi M. A numerical approach for analyzing quantum dotinfrared photodetectors' parameters[J]. *Optics & Laser Technology*, 2012, **44**:572-577.

[4] Zhou D M, Weng Q C, Wang W P, *et al*. The photocurrent of resonant tunneling diode controlled by the charging effects of quantum dots [J]. *Optical and Quantum Electronics*, 2013, **45**: 687-692.

[5] Martyniuk P, Rogalski A. Insight into performance of quantum dot infrared photodetectors[J]. *Bulletin the Polish Academy of Sciences: Technical Scinences*, 2009, **57**:103-116.

[6] Lin L, Zhen H L, Li N, *et al*. Sequential coupling transport for the dark current of quantum dots-in-well infrared photodetectors[J]. *Applied Physics Letter*, 2010, **97**: 193511-1793513.

[7] Liu H, Zhang J. Performance investigations of quantum dots infrared photodetector[J]. *Infrared physics & Technology*, 2012, **55**: 320-325.

[8] Mahmoud I I, Konder H A, El_Tokhy M S. Performance improvement of quantum dot infrared photodetectors through modelling[J]. *Optics & Laser Technology*, 2010, **42**:1240-1249.

[9] Movaghar B, Tsao S, Abdollahi Pour S, *et al*. Gain and recombination dynamics in photodetectors made with quantum nanostructures: the quantum dot in a well and the quantum well[J]. *Physical Review B*, 2008, **78**:115320-1-10.

[10] Liu H C. quantum dot infrared photodetector[J]. *Opto-electronics. Review*, 2003, **11**:1-5.

[11] Liu H C. Quantum well infrared photodetector physics and novel devices[J]. *Semiconductors and Semimetals*, 2000, **62**:126-196.

[12] Ryzhii V, Khmyrova I, Pipa V, *et al*. Device model for quantum dot infrared photodetectors and their dark current characteristics[J]. *Semiconductor Science and Technology*, 2001, **16**:331-338.

[13] Lin S, Tsai Y, Lee S. Comparison of InAs/GaAs quantum dot infrared photodetector and GaAs/(AlGa)As superlattice infrared photodetector [J]. *Japanese Journal of Applied Physics*, 2001, **40**: L1290-L1292.

[14] Ariyawansa G, Matsik S G, Perera A G U, *et al*. Tunneling quantum dot sensors for multi-band infrared ang terahertz radiation detection [C]. In: *IEEE Sensors* 2007 *Conference*, Georgia, USA, 2007: 503-506.